Supporting Information for:

Memory Effects in Compound-Specific D/H Analysis by GC/P/IRMS

Ying Wang, Alex L. Sessions*

Department of Geological and Planetary Sciences, California Institute of Technology

Address: Department of Geological and Planetary Sciences, California Institute of Technology, 1200 East California Blvd, Mail Code 100-23, Pasadena, CA 91125.

E-mail: ywjojo@gps.caltech.edu

Phone: (626)395-6894

Content:

1. Model description and typical output
2. Mathematical derivation of partitioning algorithms

* Author to whom correspondence should be addressed

1. Model description and typical output

The reactor is modeled as a linear series of discrete gas parcels moving past and interacting with a single, stationary box representing surface adsorption sites in graphitic carbon (Fig. S-1). Each gas parcel equilibrates with the graphite surface for one residence time (τ, typically 0.5 s), after which the gas parcels shift sequentially and the next gas parcel equilibrates. The molar amount and isotopic composition of hydrogen in the graphite phase are retained from one gas parcel to the next. Our model is thus conceptually similar to simple models of chromatographic partitioning between mobile and stationary phases[1]. Concentrations and isotopic compositions are assumed to be homogeneous within each gas parcel, and within the graphite 'box'. This approach is justified because at a typical GC flow of 1.2-1.5 ml/min, each gas parcel takes < 0.5 s to go through a pyrolysis reactor of 30 cm length, in which the pyrolytic carbon covers only 5-8 cm near the upstream end. Thus the timescale for interaction between H_2 gas and adsorption sites within the reactor is much shorter than typical peak width (~20 s). For similar reasons, diffusion within and between gas parcels and the graphite surface is ignored in the model. Potential consequences of these simplifications are discussed in the paper.

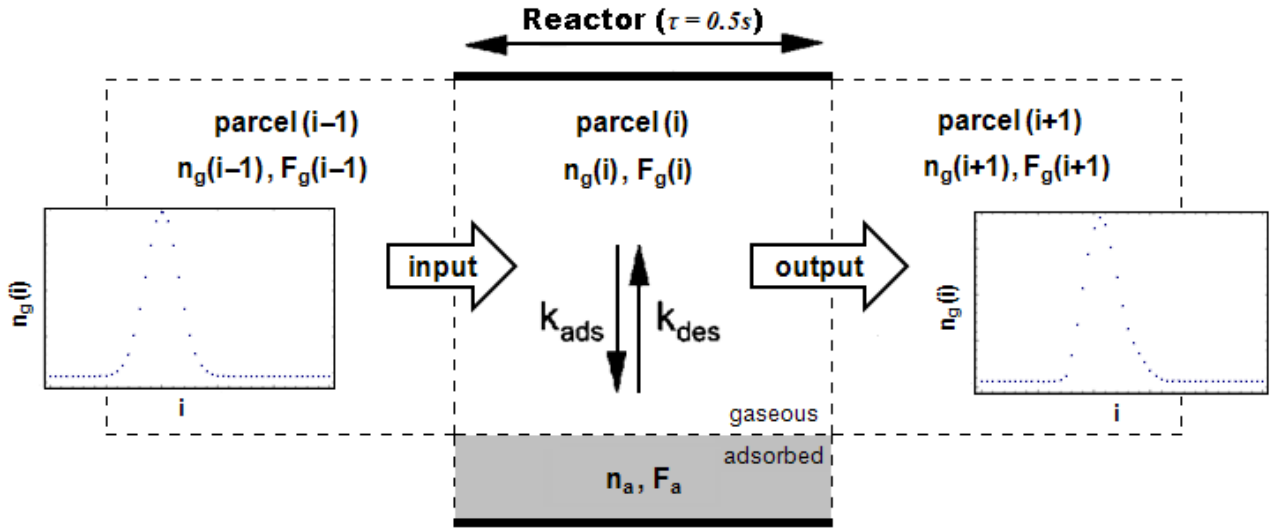

Figure S-1. Schematic description of the model, showing the equilibration of discrete gas parcels with the graphite surface pool. Also shown are sample input and output chromatograms, plotted as $n_g(i)$ vs. i.

In the model, the molar amount of hydrogen (n) and fractional deuterium abundance (F = [D]/[D+H]) are tracked for each gas parcel ($n_g(i)$, $F_g(i)$) and for the graphite surface (n_a, F_a). n_g is calculated from the product of the parcel volume (each equal to the pyrolysis reactor volume) and P_{H2}

due to analytes plus background hydrogen. These parameters can be adjusted to simulate GC peaks of varying size, shape, and temporal separation superimposed on a background of fixed size. F_g is calculated by mass balance from the stipulated δD values of the analyte (assuming no chromatographic separation of isotopes) and background hydrogen. The number of total graphite adsorption sites (N_a) is constant in the model, and is calculated from typical parameters for graphite as described in the Methods section. As each gas parcel equilibrates with the graphite surface, partitioning of both H and D between adsorbed and gaseous phases is calculated as a function of residence time (τ) using one of two algorithms, depending on whether the model is simulating weak or strong adsorption sites on the graphite. Adsorption on the two types of sites is not modeled simultaneously. We assume no isotopic fractionation during the partitioning of H_2 between adsorbed and gaseous phases.

The model produces two characteristic types of results depending on whether strong or weak adsorption sites are modeled. In the case of strong adsorption sites, graphite surface coverage remains virtually complete and so n_g and n_a do not change during equilibration. The result is that the shape of the chromatographic peak changes very little, while its isotopic composition (and that of the following background) changes substantially as a result of isotopic exchange with the pool of adsorbed hydrogen (Fig. S-2). In contrast, for weak adsorption sites the surface coverage of graphite changes with varying P_{H2} across a chromatographic peak, but quickly re-equilibrates with the background hydrogen once the peak has passed. As a result, chromatographic peaks are both broadened and delayed, while their isotopic compositions after background subtraction change very little (Fig. S-3). In effect, weak adsorption sites serve as a source of peak broadening but not of isotopic memory.

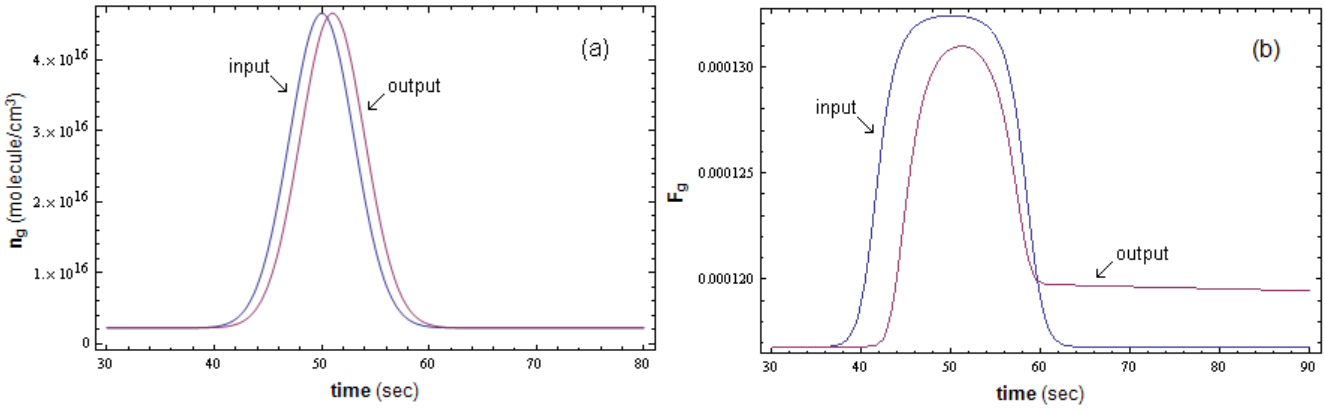

Figure S-2. Simulated input and output trace of H_2 concentration (a) and D/H ratio (b) for strong sites.

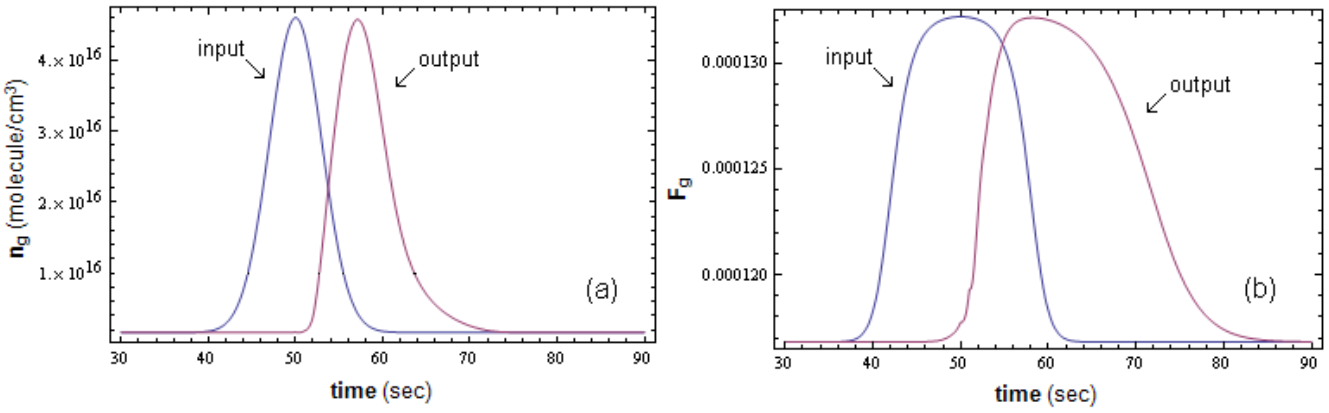

Figure S-3. Simulated input and output trace of H_2 concentration (a) and D/H ratio (b) for weak sites.

The chromatograms produced by the model were processed according to Ricci et al.[2] and Sessions[3] to obtain δD values for each peak. Specifically, peak integration intervals were evaluated based on the mass-2 chromatogram and then applied to the mass-3 chromatogram. Background was determined by the point immediately before the start of the peak and was then subtracted on a point-by-point basis across the integration interval. Because the model does not simulate the chromatographic process or the formation of H_3^+, no correction for isotope chromatography or isobaric interference is necessary. Finally, the integrated mass-2/mass-3 ratio was normalized to that of a peak (δD = -148‰) introduced 100 s before the first analyte peak, simulating the use of the CH_4 reference peak in experimental measurements.

2. Mathematical derivation of partitioning algorithms

A mathematical description for partitioning of hydrogen between the gas phase and adsorption on graphite is derived from statistical thermodynamics as follows. Assuming no chemical reactions in the vapor phase or on graphite surfaces, and that adsorption enthalpy is independent of surface coverage, the amount of adsorbed hydrogen at equilibrium obeys the Langmuir Isotherm. Equilibrium surface coverage for molecular adsorption (θ_m) and dissociative adsorption (θ_d) is expressed as:

$$\theta_m = \frac{KP}{KP+1} \qquad (S-1a)$$

$$\theta_d = \frac{\sqrt{KP}}{\sqrt{KP}+1} \qquad (S-1b)$$

where P is H_2 partial pressure at equilibrium and K is the equilibrium constant ($K = k_{ads}/k_{des}$) (ref. 4). Because K reflects equilibrium partitioning, it can be calculated from statistical thermodynamics apart

from reaction kinetics[5-7]. For the dissociative adsorption H_2 + 2S ↔ 2S-H (where S denotes a generic surface site), the value of K is given by[7]

$$K = h^3(2\pi m k_B T)^{-\frac{3}{2}}(\frac{kT}{P})^{-1}(\frac{T}{\sigma\theta_{rot}})^{-1}\frac{(1-e^{-h\nu_H/kT})}{(1-e^{-h\nu_{SH}/kT})^2}e^{-\frac{\Delta E}{kT}} \quad (S-2)$$

where h and k_B are Planck and Boltzmann constants, T is the temperature, m is molecular mass, θ_{rot} is the characteristic temperature of rotation (θ_{HH} = 88 K, θ_{HD} = 66 K; ref. 8), σ is the symmetry factor (σ_{HH} = 2, σ_{HD} = 1), and ΔE is the adsorption enthalpy. The parameters υ_H and υ_{SH} represent the vibrational frequencies for gaseous H_2 molecules (υ_{HH} = 4401 cm^{-1}, υ_{HD} = 3813 cm^{-1}; ref. 8) and for surface-bound hydrogen, respectively. The value of υ_{SH} for normal and parallel vibrations is reported as 2900 to 1450 cm^{-1} for chemisorbed hydrogen on pyrolytic graphite[9] and 1000 to 2000 cm^{-1} for hydrogen adsorbed on various surface sites of copper[10, 11]. Since the calculation is relatively insensitive to υ_{SH}, average frequencies were adopted. K for molecular adsorption has the same formulation, except that the change in vibrational entropy is assumed to be negligible. Combining eqns. S-1 and S-2, the equilibrium surface coverage can be calculated as a function of temperature, pressure and adsorption enthalpy (Fig. 6 in the paper). Two characteristic regions are recognized. When adsorption enthalpy is high (ΔE > 4.5 eV, corresponding to **'strong' adsorption sites**), surface coverage is virtually complete regardless of P_{H2}. When adsorption enthalpy is lower (1.4 < ΔE < 4.5 eV, corresponding to **'weak' adsorption sites**), surface coverage varies as a function of P_{H2}. Because of these different behaviors, the two types of adsorption sites are modeled separately.

Our model seeks to reproduce time-dependent equilibration of gas and adsorbed phases, so the kinetics of this exchange must also be considered. According to Langmuir theory, adsorption is a second-order process and its rate is proportional to the number of gaseous molecules and number of unoccupied adsorption sites:

$$\frac{dn_a}{dt} = k_{ads}n_g(1-\theta)N_a \quad (S-3)$$

where θ is the fractional surface coverage at time t. The desorption process is considered as a first-order process with the rate proportional to the number of occupied surface sites:

$$-\frac{dn_a}{dt} = -k_{des}\theta N_a \quad (S-4)$$

k_{ads} (s^{-1}molecule^{-1})and k_{des} (s^{-1}) are the adsorption and desorption rate constants. Setting eqn. S-3 equal to eqn. S-4, the fractional surface coverage at equilibrium can be obtained as[4]:

$$\theta_e = \frac{k_{ads}n_g}{k_{ads}n_g + k_{des}} \quad (S-5)$$

At any time, the molecular adsorption (f_{ads}) and desorption (f_{des}) fluxes are given by eqns. S-3

and S-4, and the corresponding adsorption and desorption fluxes of D are simply $F_g\, f_{ads}$ and $F_a\, f_{des}$ respectively. The net transfer of D between gas phase and adsorbed phase is then given by:

$$F_g f_{ads} + F_a f_{des} = F_g k_{ads} n_g (1-\theta) N_a - F_a k_{des} \theta N_a \quad (S-6)$$

where a positive value represents net transfer of D into the adsorbed phase, and a negative value represents net transfer into the gas phase. Alternatively, the net change in D content of the adsorbed phase can be written as the derivative

$$\frac{d(F_a n_a)}{dt} = n_a \frac{dF_a}{dt} + F_a \frac{dn_a}{dt} \quad (S-7)$$

Eqns. S-6 or S-7 could in theory be evaluated directly. Unfortunately, the calculation of k_{ads} contains a number of significant uncertainties, so we adopted several further simplifications.

(i) Strong adsorption sites. For strong adsorption sites, surface sites are nearly saturated regardless of P_{H2}. Thus n_a is constant and $dn_a/dt = 0$. Combining S-6 and S-7, we get:

$$\frac{d(F_a n_a)}{dt} = n_a \frac{dF_a}{dt} = F_g k_{ads} n_g (1-\theta) N_a - F_a k_{des} \theta N_a \quad (S-8)$$

which, by substituting $n_a = N_a \times \theta$, can be simplified to

$$\frac{dF_a}{dt} = F_g k_{ads} n_g \left(\frac{1}{\theta} - 1\right) - F_a k_{des} \quad (S-9)$$

Although the pool of adsorbed hydrogen equilibrates very slowly with H_2 in the gas phase due to the large desorption energy ($t_{1/2} > 10^0$ s), both θ_e and θ are very close to 1 and thus $\theta \approx \theta_e$. Therefore eqn. S-5 can be applied to further simplify eqn. S-9 to:

$$\frac{dF_a}{dt} = k_{des}(F_g - F_a) \quad (S-10)$$

Following a similar approach, the net change in fractional abundance of D in the gas phase can be obtained as

$$\frac{dF_g}{dt} = -\frac{n_a}{n_g} k_{des}(F_g - F_a) \quad (S-11)$$

The differential eqns. S-10 and S-11 can then be solved to give F_g and F_a as functions of time:

$$F_g(t) = \frac{(F_g^0 - F_a^0) n_a}{n_a + n_g} e^{-k_{des}\left(1+\frac{n_a}{n_g}\right)t} + \frac{F_g^0 n_g + F_a^0 n_a}{n_g + n_a} \quad (S-12)$$

$$F_a(t) = \frac{(F_a^0 - F_g^0) n_g}{n_a + n_g} e^{-k_{des}\left(1+\frac{n_a}{n_g}\right)t} + \frac{F_g^0 n_g + F_a^0 n_a}{n_g + n_a} \quad (S-13)$$

in which a superscript '0' reflects the fractional abundance prior to equilibration. In the model, eqns. S-12 and S-13 are used to calculate changes in the isotopic composition of gaseous and adsorbed hydrogen at time $t = \tau$. There is no change in the abundance of hydrogen in either phase because – for strong adsorption sites – surface coverage remains complete. The rate of isotopic exchange is controlled by k_{des}

and the relative sizes of the two hydrogen pools.

(ii) Weak adsorption sites. For weak adsorption sites, n_a varies substantially with P_{H2} as a result of changing surface coverage, and thus the above simplifications for strong sites do not apply. We therefore took an alternative approach. Because the desorption half-life for weak sites is much shorter than τ, hydrogen exchange between the gas and graphite phases achieves equilibrium almost instantaneously. Thus for each gas parcel we can first calculate the equilibrium partitioning of hydrogen between adsorbed and gas phases (i.e., θ^e) using $n_g{}^0$ as input to eqn. S-5. The superscript '0' again indicates the value prior to equilibration. In this case, application of eqn. S-5 is approximate because $n_g{}^e$ (i.e., at equilibrium) will vary with θ_e, and vice-versa, as there is a net transfer of hydrogen to or from the adsorbed phase. Although an exact solution for $n_g{}^e$ and θ^e is possible through an iterative calculation, such an approach is not warranted here because the errors introduced are negligible given that changes in $n_g{}^0$ from one gas parcel to the next are quite small. The new (equilibrium) hydrogen amount in the adsorbed phase can then be computed as $n_a{}^e = \theta^e N_a$, and the equilibrium amount of hydrogen in the gas phase computed as

$$n_g{}^e = n_g{}^0 + (n_a{}^0 - n_a{}^e) \qquad (S-14)$$

Calculation of the fractional abundance of D in the adsorbed and gas phases is based on isotopic mass balance. The total abundance of D in the gas + adsorbed phases must remain constant during equilibration:

$$n_g{}^0 F_g{}^0 + n_a{}^0 F_a{}^0 = n_g{}^e F_g{}^e + n_a{}^e F_a{}^e \qquad (S-15)$$

Recognizing that $F_g{}^e = F_a{}^e$ at equilibrium because we assume no isotopic fractionation during the partitioning, and that $n_g{}^0+n_a{}^0=n_g{}^e+n_a{}^e$, eqn. S-15 can be rearranged to give the equation employed by the model:

$$F_g{}^e = F_a{}^e = \frac{F_g^0 n_g + F_a^0 n_a}{n_g{}^0 + n_a{}^0} \qquad (S-16)$$

REFERENCE

(1) Peters, D. G. H., J. M.; Hieftje, G. M. *Chemical Separations and Measurements: Theory and Practice of Analytical Chemistry* W.B. Saunders Company, 1974.

(2) Ricci, M. P.; Merritt, D. A.; Freeman, K. H.; Hayes, J. M. *Organic Geochemistry* **1994**, *21*, 561-571.

(3) Sessions, A. L. *Journal of Separation Science* **2006**, *29*, 1946-1961.

(4) Billing, G. D. *Dynamics of molecular surface interactions*; John Willy & Sons. Inc., 2000.

(5) Fowler, R. H. *Proceedings of the Cambridge Philosophical Society* **1935**, *31*, 260-264.

(6) Fowler, R. H. *Proceedings of the Cambridge Philosophical Society* **1936**, *32*, 144-151.

(7) Hoinkis, E. *Journal of Nuclear Materials* **1991**, *182*, 93-106.

(8) Computational Chemistry Comparison and Benchmark DataBase, National Institute of Standards and Technology, 2006.

(9) Zecho, T.; Guttler, A.; Sha, X. W.; Jackson, B.; Kuppers, J. *Journal of Chemical Physics* **2002**, *117*, 8486-8492.

(10) Lee, G.; Plummer, E. W. *Surface Science* **2002**, *498*, 229-236.

(11) McCash, E. M.; Parker, S. F.; Pritchard, J.; Chesters, M. A. *Surface Science* **1989**, *215*, 363-377.